Synthesis of Nanosized Pd/CNT Catalyst by *m*-Chloroperbenzoic Acid Oxidation Method and Catalytic Hydrogenation Reaction

JONG-GEUN CHOI, CHONG-YEON PARK and WON-CHUN OH*

Department of Advanced Materials Science & Engineering, Hanseo University, Seosan-si, Chungnam 356-706, South Korea

*Corresponding author: Fax: +82 41 6883352; Tel: +82 41 6601337; E-mail: wc_oh@hanseo.ac.kr

Palladium nanoparticles (4-10 nm) were deposited outside multi-walled carbon nanotubes (MWCNTs) by *m*-chloroperbenzoic acid (MCPBA) oxidation method using an aqueous solution containing a palladium salt. The MCPBA oxidation method was extremely efficient as palladium particle located on the outer surface of the tubes was observed. The dispersion and structure of the palladium in the synthesized Pd/CNT catalyst determined by X-ray diffraction (XRD), energy dispersive X-ray (EDX) spectroscopy, scanning electron microscopy (SEM) and transmission electron microscopy (TEM). The catalyst was tested for the selective hydrogenation of cinnamaldehyde by gas chromatography. The carbon nanotubes based catalyst exhibits along with a high catalytic activity an extremely high selectivity towards the C=C bond hydrogenation.

Key Words: Carbon nanotubes, Palladium, Transmission electron microscopy, *m*-Chloroperbenzoic acid, Hydrogenation.

INTRODUCTION

Nanoparticle (NP)/carbon nanotube (CNT) composites have attracted much attention due to their potential utility[1], anode materials in lithium-ion batteries[2], sensors of DNA hybridization[3], hydrogen storage[4,5], catalytic hydrogenation[6] and electrocatalysts[7]. Several methods have been proposed to prepare these composites, such as electroless plating[8], electrochemical deposition[9,10], solid state reaction[11] and chemical deposition[12,13]. For many applications, it is necessary to functionalize their surfaces to obtain higher performances. And, it has been shown that functionalization should be performed to produce well dispersed supported catalysts[14]. Among the many processes for carbon nanotube surface functionalization[15], fluorination and the introduction of oxygenated groups such as carboxyl, hydroxyl and carbonyl groups are the most frequently used, due to the simplicity and feasibility of the relevant reactions involved and of further reactions after these treatments. The first studies on the functionalization of carbon nanotube from the middle of the 90's have been largely inspired on the methods used for oxidation of many kinds of carbon materials. The most common method is based on liquid phase oxidation by concentrated nitric acid or sulfuric acid/nitric acid mixtures, which was used mainly for surface oxidation of carbon materials[16-19], but also of MWCNT or SWCNT[20-25]. This oxidation procedure generally leads to the opening of ring of carbon nanotubes ends and the production of carboxyl, hydroxyl and carbonyl groups.

Recently, carbon nanotubes (CNTs) have received considerable attention as catalyst supports in both heterogeneous catalysis and electrocatalysis due to their high mechanical strength, large surface area, good electrical conductivity and durability under harsh conditions[26], which makes them interesting to promote a variety of liquid-phase reactions such as methanol oxidation, hydrogenation and dehydrogenation of organics[27]. Furthermore, specific metal-combined interactions exist in carbon nanotube based solids that can directly affect the catalytic activity and the selectivity. Some researchers have reported carbon nanotube-supported catalysts (*e.g.*, Pt, Pd, Au_2, Ru and RuO_2) exhibiting good catalytic behaviors under various chemical reaction conditions, involving electro-oxidation[28], selective hydrogenation[29]. Among these metals, Pt and Pd group metals are considered to be the most frequently employed catalyst materials for the chemical and electrochemical reactions. Recently, palladium catalysts supported on multi-walled carbon nanotubes were tested for catalytic liquid-phase alcohol oxidation[30]. The roll of Pd on Pd/CNT have a function to dissociate hydrogen easily penetrate into the interlayers and hollow interiors of carbon nanotubes. Hydrogen atoms/protons could bond with carbon atoms by chemisorption or charge transfer and form hydrogen molecules in tubes. It is expected that specific properties will be observed with these

combined nanomaterials, especially in the heterogeneous catalysis field, compared to those usually encountered with traditional catalysts such as powders, grains and extrudates. The introduction of foreign elements inside or outside the nanotube may modify the physical and chemical properties of the combined material.

The goal of the present work is to study of oxidation on multi-walled carbon nanotubes (MWCNTs) by *m*-chloro-perbenzoic acid (MCPBA) method and to evaluate the influence of this treatment on the catalytic performance of Pd/MWCNT catalyst for selective hydrogenation. Results of catalytic performance are discussed along with catalyst characterization by X-ray powder diffraction (XRD), scanning electron microscopy (SEM), transmission electron microscopy (TEM) and energy dispersive X-ray (EDX). This catalyst was tested in the selective hydrogenation of cinnamaldehyde to cinnamyl alcohol by gas chromatography.

EXPERIMENTAL

Carbon nanotubes (CNTs) were selected as the support material. The carbon nanotubes (multi-walled carbon nanotubes, diameter: *ca.* 20 nm, length: *ca.* 5 µm) were supplied by Carbon Nano-Material Technology Co. (Korea) and used without further purification. For the oxidization the surface of carbon nanotube, *m*-chloroperbenzoic acid (MCPBA) was used as an oxidizing reagent which was purchased from Acros Organics, New Jersey, USA. Hydrogen hexachloropalladinate (IV) hydrate ($H_2PdCl_6 \cdot 6H_2O$) was obtained from Kojima Chemical Co. Ltd. Reagents (benzene and ethylene glycol) were purchased as reagent-grade from Duksan Pure Chemical Co. and Daejung Chemical Co. and used without further purification.

Preparation of Pd/CNT catalyst: The oxidized carbon nanotubes were added to ethylene glycol solution containing 0.5M $H_2PdCl_6 \cdot 6H_2O$ and then the solution was homogenized under reflux at 343 K for 2 h using a magnetic stirrer in a vial. After being heat treated at 773 K for 1 h with a heating rate of 275.8 K/min, the Pd treated carbon nanotube catalyst was obtained.

Characterization of Pd/CNT catalyst: XRD technique was used for crystal phase identification. XRD patterns were obtained at room temperature with a diffractometer Shimata XD-D1 (Japan) using Cu K_α radiation. SEM (Jeol, JSM-5200, Japan) was used to observe the surface state and porous structure of the Pd/carbon nanotube catalyst. EDX spectroscopy was used to measure the elemental analysis of the Pd/CNT catalyst. TEM (Jeol, JEM-2010, Japan) at an acceleration voltage of 200 kV was used to investigate the size and distribution of the Pd on the carbon nanotube surface of sample. TEM specimens were prepared by placing a few drops of the sample solution on a carbon grid.

Catalytic test of cinnamaldehyde: The catalytic hydrogenation of cinnamaldehyde was carried out in the slurry reactor under atmospheric pressure condition at ambient temperature. Before reaction, the Pd/CNT catalyst (0.08 g) was *in situ* added at 50 ºC for 3 h. 5 mL of cinnamaldehyde dissolved in 30 mL of dioxane are injected into three-necked bottle with 0.08 g catalyst. Hydrogen gas (15 mL/min) was

continuously fed into the reactor *via* a mass flow controller under stirring at 500 rpm. A small amount of (0.3 mL) of the reacting medium was withdrawn intermittently at regular times and analyzed by gas chromatography (GC HP5973, Hewlett-Packard) equipped with capillary column (Carbobond with 50 m in length) and FID detector.

RESULTS AND DISCUSSION

Structure and morphology of Pd/CNT catalyst: The powder XRD patterns of pristine carbon nanotube and Pd/CNT catalyst are shown in Fig. 1. The strong and small peaks at $2\theta = 26.5º$, 42.4º and 44.6º are attributed to the hexagonal graphite structure (002), (100) and (101), which suggests carbon nanotube has a high graphite structure and good electrical conductivity[31]. However, the medium peak at 36.5º is derived from Fe element as impurity. The Pd diffraction peaks show that the catalyst has a face centered cubic (fcc) crystal structure. The diffraction peaks at $2\theta = 40.1º$, 46.5º and 68.0º can be assigned to Pd (111), (200) and (220) diffraction peaks, respectively.
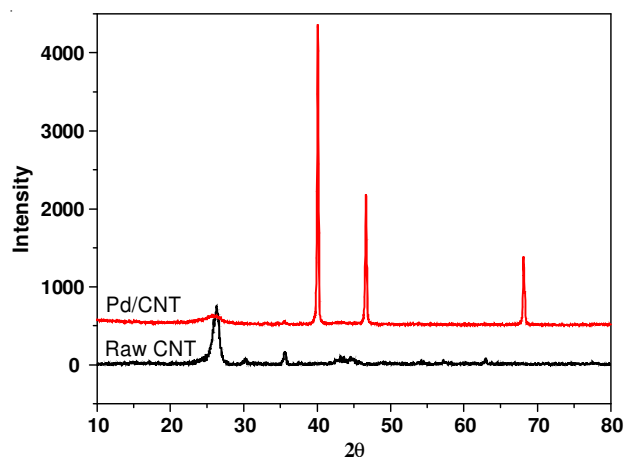

Fig. 1.   X-ray diffraction pattern of palladium particles introduced MWCNT (Pd/CNT)

The micro-surface structures and morphology of the Pd/CNT catalyst were characterized by SEM. Typical SEM images of Pd/CNT are shown in Fig. 2. As shown in Fig. 2, the Pd particles were well dispersed to the surface of the carbon nanotube network, but the detail distribution was not distinguishable. According to the Tessonnier *et al.*[32], a good dispersion of nanosized small particles could provide better reactivity with a reactant than aggregated particles. Pd/CNT catalyst has porous and three-dimensional structure. The three-dimensional structure, smaller particle size and high dispersion of nanosized particles may result in large valuable Pd surface area and good catalytic properties towards cinnamaldehyde.

Fig. 3 illustrates the representative TEM micrographs of Pd/CNT prepared by MCPBA oxidation method. The TEM images of the reduced sample are presented in Fig. 3(a-b). Low magnification TEM image clearly shows that all the palladium particles were located outside the carbon nanotubes [Fig. 3(a-b)] shows that well-dispersed Pd particles were homogeneously anchored on the external walls of the carbon nanotubes. The particle-size of Pd distributed in a narrow
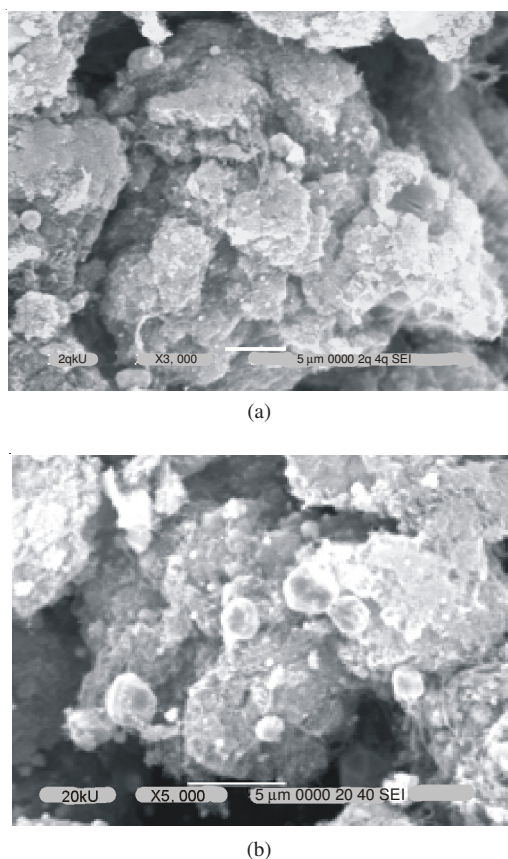
(a)

(b)

Fig. 2. SEM images of the palladium particles introduced MWCNT (Pd/CNT); (a) low magnification (× 3000) and (b) high magnification (× 5000)
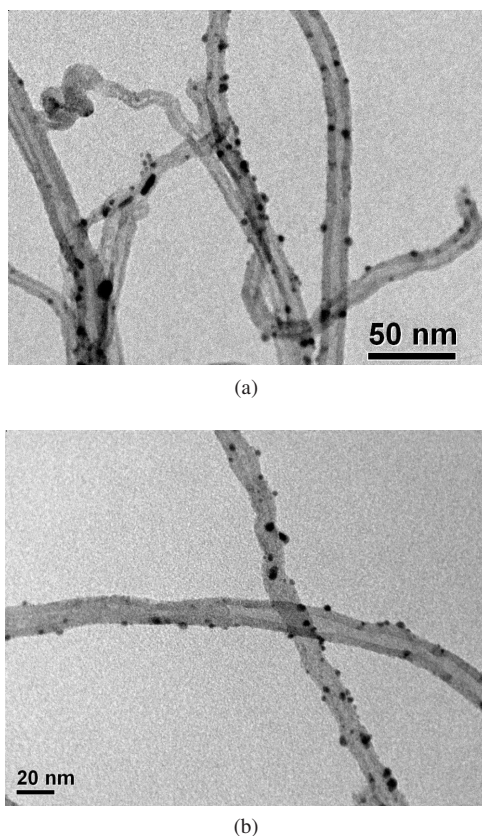

(a)

(b)

Fig. 3. TEM images of the palladium particles introduced MWCNT (Pd/CNT); (a) large scale (50 nm) and (b) small scale (20 nm)

range (4-6 nm). According to the previous work[33], the wide nanotube cavities appeared to be more preferentially filled compared to the narrower cavities. In small cavities, the van der Waals repulsion forces are significantly higher than that of capillarity and thus inhibit the penetration of the solution inside the tube channel. In the present work, the almost absence of any palladium particles on the outer surface of the tube is concerned to the relatively small inner cavity and the relatively metal precursor concentration due to the hydrophobic character of the outer surface of the nanotubes [Fig. 3(b)]. Detail examination of the TEM image indicates that the palladium particles shape was faceted which could be due to a strong metal-support interaction with the outer wall surface of the carbon nanotubes. Such a relatively high interaction could give rise to the relatively high dispersion of the palladium particles with the different thermal treatments steps. The relatively high interaction between the deposited palladium and the outer wall surface of the carbon nanotubes could come from the electronic modification by oxidation of the graphene planes. The presence of structural defects on the tube wall and surface could also induced anchorage of the active phase particles on the wall and surface. It is described that the degree of dispersion is corresponding to the reactivity of flat interface between the metal particle and the outer tube surface with disordered graphene planes. The nature of the palladium precursor salt has almost no detected effect on the final dispersion state of the metallic particles. Statistical measurements performed on metallic Pd particles on the carbon nanotube surface lead to an average particle size distribution centered at around 5 ± 1 nm despite of the presence in some areas of the catalyst of relatively large palladium particles with a size close to 10 nm (Fig. 4).
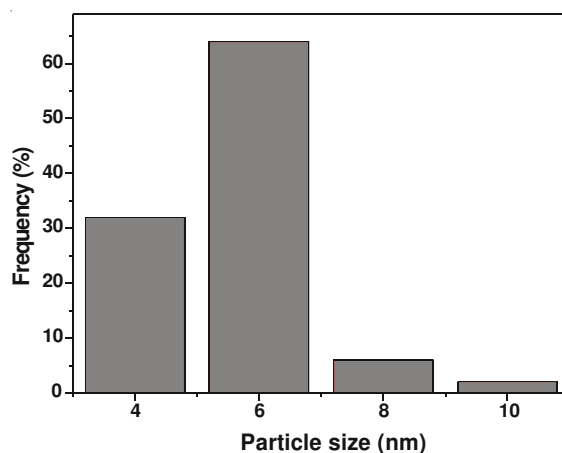

Fig. 4. Average palladium size deduced from statistical TEM results about Pd/CNT

The result of the EDX elemental microanalysis of the Pd/CNT catalyst has been investigated by EDX and its corresponding image was shown in Fig. 5. The elemental contents of the carbon, oxygen and palladium for Pd/CNT are 63.4, 6.33 and 21.6 %, respectively. It can be expected that the amounts of palladium is satisfied with catalytic reactivity for hydrogenation reaction of organic compounds.
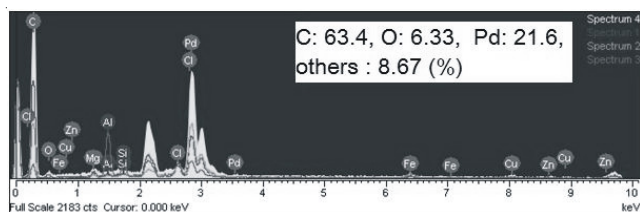
Fig. 5. EDX elemental microanalysis of Pd/CNT catalyst

C: 63.4, O: 6.33, Pd: 21.6, others : 8.67 (%)

Hydrogenation catalytic activity: Catalytic selective hydrogenation of organic compounds is crucial manufacturing process in the refinery of petrochemical and chemicals. The catalytic metallic components generally used in these kinds of reactions are palladium and platinum. The main reaction pathway for the selective hydrogenation of cinnamaldehyde is shown in Fig. 6. The hydrogenation of cinnamaldehyde leads to the reduction of carbonyl groups, unsaturated aromatic and aliphatic compounds parallel and consecutive reduction of different functional groups present in the C=C and C=O bonds to the production of the unsaturated cinnamyl alcohol (I). An alternative route involves the reduction of the olefinic C=C bond leading to saturated hydrocinnamaldehyde (II). Additionally, both cinnamyl alcohol (I) and hydrocinna-maldehyde (II) can be further progress of hydrogenation to produce the completely saturated hydrocinnamyl alcohol (III). The catalytic activity obtained from Pd/CNT catalyst is depicted in Fig. 7. The results clearly observed the decrease of the amounts of cinnamaldehyde with an increase of amount of hydrocinnamaldehyde (II) and hydrocinnamyl alcohol (III) as time function. The excellent activity of Pd/CNT catalyst is mainly related to the homogeneous distribution of ultrafine metallic palladium particles over carbon nanotube surfaces. The influence of surface groups in carbon supported catalysts received the increase of attention[34-37]. And, it has been reported that, for α, β-unsaturated aldehydes hydrogenation on monometallic catalysts, their removal provides for more active materials and increases selectivity towards the saturated aldehyde[34-36]. The high external surface area of the carbon nanotubes allowed a significant decrease in the mass transfer limitation, which is predominant in liquid-phase reactions, since the transport of the reactants from the bulk of the liquid to the external surface of the catalyst is strongly dependent in the size of the pores of the catalyst. The difference in the selectivity could be attributed to several factors: (i) the existence of a peculiar metal-support interaction between the palladium metal crystallites and the carbon nanotubes surface in the inner cavity, *i.e.*, electronic modification through the electron transfer between the metal and the support, which in turn modifies the adsorption and selectivity of the products[38,39], (ii) the complete absence of any microporosity, which could modify the residence time of the reactants and products and their adsorption properties and (iii) the low concentration of oxygenated groups on the carbon nanotube surface could also influence in a significant manner the catalytic selectivity by modifying the adsorption mode of the reactant. Toebes *et al.*[40], have recently reported that the hydrocinnamaldehyde formation can be highly enhanced by removing the oxygenated groups present on the Pt/CNF catalyst. Finally, it should be stressed that the presence of residual acidity on the carbon
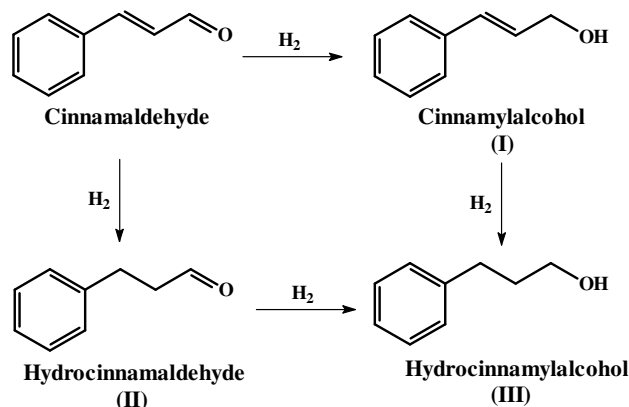

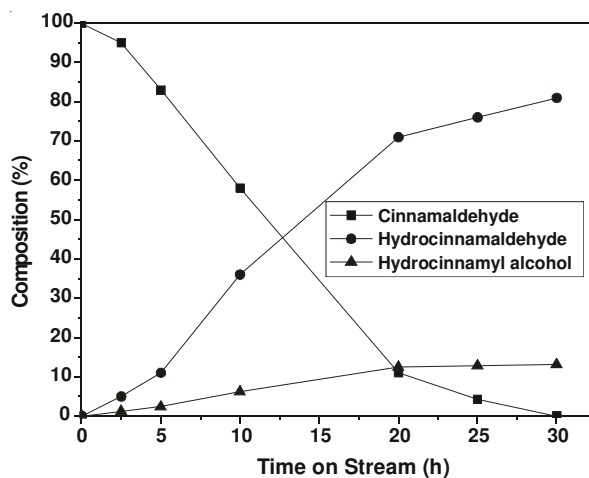Fig. 6. Reaction pathway for the selective hydrogenation of cinnamaldehyde

Fig. 7. Catalytic activity for the selective hydrogenation of cinnamaldehyde into hydrocinnamaldehyde over Pd/CNT catalyst at atmospheric pressure condition at ambient temperature in a liquid-phase medium

surface could also modify the hydrogenation pathway leading to a selective catalyst. It should also be noted that an interaction would be also possible between the C=C bond of the substrate and the exposed basal plane associated with a cloud of delocalized π-electrons of the support. Elemental analysis carried out on the filtered solution reveals no trace of palladium species, which indicate that leaching phenomenon if present was negligible. The hydrocinnamaldehyde was not further reduced on catalysts under the reaction conditions employed, which indicates that the re-adsorption of the molecule through the C=O bond did not occur on the palladium site regardless of the nature of the support. The observed result indicates that on the Pd/CNTs catalyst the C=C hydrogenated product was rapidly desorbed from the active site. And, the cinnamaldehyde was adsorbed in a different way leading to the almost simultaneous hydrogenation of the C=O and C=C bonds without desorption of the C=O hydrogenated intermediate. Such adsorption mode could be directly linked to the electronic state of the metallic active site.

Conclusion

In this study, palladium metal nanoparticles can be easily introduced in the carbon nanotubes by a *m*-chloroperbenzoic acid oxidation method followed by classical thermal

treatments. XRD data revealed that the structure for the Pd/CNT catalyst showed a face centered cubic (fcc) crystal structure. The SEM and TEM microphotographs of Pd/CNT catalyst showed that nanosized Pd particles were distributed uniformly in the carbon nanotubes network and the Pt particles were fixed on the surface of the carbon nanotubes. The metallic Pd particles on the carbon nanotube surface lead to an average particle size distribution centered at around 5 ± 1 nm. The presence of a confinement effect induced by the carbon nanotube wall during the thermal treatment has probably a strong influence on the formation of these small metal particles. This catalyst exhibits a high selectivity towards the C=C bond hydrogenation, which could be attributed to the peculiar morphology of the support. And, the excellent activity of Pd/CNT catalyst is mainly related to the homogeneous distribution of ultrafine metallic palladium particles over carbon nanotube surfaces.

REFERENCES

1. P.C. Ma, B.Z. Tang and J.K. Kim, *Carbon*, **46**, 1497 (2008).
2. J. Yan, H. Song, S. Yang, J. Yan and X. Chen, *Electrochim. Acta*, **53**, 6351 (2008).
3. M. Gao, H. Qi, Q. Gao and C. Zhang, *Electroanalysis*, **20**, 123 (2007).
4. Y. Suttisawat, P. Rangsunvigit, B. Kitiyanan, M. Williams, P. Ndungu, M.V. Lototskyy, A. Nechaev, V. Linkov and S. Kulprathipanja, *Hydrogen Energy*, **34**, 6669 (2009).
5. R. Campesi, F. Cuevas, R. Gadiou, E. Leroy, M. Hirscher, C. Vix-Guterl and M. Latroche, *Carbon*, **46**, 206 (2008).
6. A. Solhy, B.F. Machado, J. Beausoleil, Y. Kihn, F. Goncalves, M.F.R. Pereira, J.J.M. Orfao, J.L. Figueiredo, J.L. Faria and P. Serp, *Carbon*, **46**, 1194 (2008).
7. G.W. Yang, G.Y. Gao, C. Wang, C.L. Xu and H.L. Li, *Carbon*, **46**, 747 (2008).
8. Y. Feng and H. Yuan, *J. Mater. Sci.*, **39**, 3241 (2004).
9. Y.F. Ding, G.P. Jin and J.G. Yin, *Chin. J. Chem.*, **25**, 1094 (2007).
10. Y.C. Chen, R.J. Young, J.V. Macpherson and N.R. Wilson, *J. Phys. Chem. C*, **111**, 16167 (2007).
11. B. Xue, P. Chen, Q. Hong, J.Y. Lin and K.L. Tan, *J. Mater. Chem.*, **11**, 2378 (2001).
12. B.C. Satishkumar, E.M. Vogl, A. Govindaraj and C.N.R. Rao, *J Phys. D: Appl. Phys.*, **29**, 3173 (1996).
13. D.J. Guo and H.L. Li, *Carbon*, **43**, 1259 (2005).
14. P. Serp, M. Corrias and P. Kalck, *Appl. Catal. A*, **253**, 337 (2003).
15. D. Tasis, N. Tagmatarchis, A. Bianco and M. Prato, *Chem. Rev.*, **106**, 1105 (2006).
16. W.C. Oh and C.S. Lim, *J. Ceramic Process. Res.*, **7**, 95 (2006).
17. P.V. Lakshminarayanan and H. Toghiani, *Carbon*, **42**, 2433 (2004).
18. J. Li, M.J. Vergne, E.D. Mowles, W.-H. Zhong, D.M. Hercules and C.M. Lukehart, *Carbon*, **43**, 2883 (2005).
19. A. Rasheed, J.Y. Howe, M.D. Dadmun and P.F. Britt, *Carbon*, **45**, 1072 (2007).
20. C.N.R. Rao, A. Govindaraj and B.C. Satishkumar, *Chem. Commun.*, **15**, 25 (1996).
21. M.S.P. Shaffer, X. Fan and A.H. Windle, *Carbon*, **36**, 1603 (1998).
22. T. Saito, K. Matsushige and K. Tanaka, *Physica B*, **323**, 280 (2002).
23. A. Kuznetsova, I. Popova, J.T. Yates, M.J. Bronikowski, C.B. Huffman, J. Liu, R.E. Smalley, H.H. Hwu and J.G. Chen, *J. Am. Chem. Soc.*, **123**, 10699 (2001).
24. T.I.T. Okpalugo, P. Papakonstantinou, H. Murphy, J. McLaughlin and N.M.D. Brown, *Carbon*, **43**, 153 (2005).
25. Z. Yu and L.E. Brus, *J. Phys. Chem. A*, **104**, 10995 (2000).
26. T.-J. Zhao, D. Chen, Y.-C. Dai, W.-K. Yuan and A. Holmen, *Top Catal.*, **45**, 87 (2007).
27. C.D. Taboada, J. Batista, A. Pinter and J. Levec, *Appl. Catal. B: Environ.*, **89**, 375 (2009).
28. Z. Yu, Ø. Borg, D. Chen, E. Rytter and A. Holmen, *Top Catal.*, **45**, 69 (2007).
29. R.V. Hull, L. Li, Y. Xing and C.C. Chusuei, *Chem. Mater.*, **18**, 1780 (2006).
30. A. Villa, D. Wang, N. Dimitratos, D. Su, V. Trevisan and L. Prati, *Catal. Today*, **150**, 8 (2010).
31. P.J.F. Harris, Carbon Nanotube Science; Preparation Properties and Applicatios, Cambridge University Press, pp. 147-178 (2009).
32. J.P. Tessonnier, L. Pesant, G. Ehret, M.J. Ledoux and C. Pham-Huu, *Appl. Catal. A: Gen.*, **288**, 203 (2005).
33. D. Ugarte, A. Chatelain and W.A. de Heer, *Science*, **274**, 1897 (1996).
34. F. Coloma, A. Sepulveda-Escribano, J.L.G. Fierro and F. Rodrýguez-Reinoso, *Appl. Catal. A Gen.*, **150**, 165 (1997).
35. M.L. Toebes, F.F. Prinsloo, J.H. Bitter, A.J. van Dillen and K.P. de Jong, *J. Catal.*, **214**, 78 (2003).
36. M.L. Toebes, Y. Zhang, J. Hajek, T.A. Nijhuis, J.H. Bitter and A.J. van Dillen, *J. Catal.*, **226**, 215 (2004).
37. H. Vu, F. Goncalves, R. Philippe, E. Lamouroux, M. Corrias and Y. Kihn, *J. Catal.*, **240**, 18 (2006).
38. R. Schlogl, In eds.: F. Schuth, K.S.W. Sing and J. Weitkamp, Surface Composition and Structure of Active Carbon, Handbook of Porous Solids, Wiley-VCH, pp. 1863-1900 (2002).
39. C. Pham-Huu, N. Keller, G. Ehret and M.J. Ledoux, *J. Catal.*, **200**, 400 (2001).
40. M.L. Toebes, Y. Zhang, J. Hajek, T.A. Nilhuis, J.H. Bitter, A.J. van Dillen, D.Y. Murzin, D.C. Koningsberger and K.P. de Jong, *J. Catal.*, **226**, 215 (2004).